

# Synthesis of diblock copolymers consistent of POSS-containing random methacrylate copolymers and polystyrene and their cross-linked microphase-separated structure via fluoride ion-mediated cage scrambling

*Kousuke Tsuchiya, Yoshihito Ishida, and Atsushi Kameyama*

Department of Chemistry, Kanagawa University, 3-27-1 Rokkakubashi, Yokohama-shi, Kanagawa 221-8686, Japan. E-mail: kameya01@kanagawa-u.ac.jp.

## Table of Contents

<b>Fig. S1</b> <sup>1</sup> H NMR spectrum of PMAPhPOSS ( <b>P1</b> ) in CDCl <sub>3</sub> .	... p1
<b>Fig. S2</b> <sup>1</sup> H NMR spectrum of P(MAPhPOSS- <i>r</i> -MMA) ( <b>P2</b> ) in CDCl <sub>3</sub> .	... p1
<b>Fig. S3</b> <sup>1</sup> H NMR spectrum of P(MAPhPOSS- <i>r</i> -MMA) ( <b>P4</b> ) in CDCl <sub>3</sub> .	... p2
<b>Fig. S4</b> <sup>1</sup> H NMR spectrum of P(MAPhPOSS- <i>r</i> -DEGMA) ( <b>P5</b> ) in CDCl <sub>3</sub> .	... p2
<b>Fig. S5</b> <sup>1</sup> H NMR spectrum of P(MAPhPOSS- <i>r</i> -HEMA) ( <b>P6</b> ) in CDCl <sub>3</sub> .	... p3
<b>Fig. S6</b> <sup>1</sup> H NMR spectrum of PMAPhPOSS- <i>b</i> -PSt ( <b>B1</b> ) in CDCl <sub>3</sub> .	... p3
<b>Fig. S7</b> <sup>1</sup> H NMR spectrum of P(MAPhPOSS- <i>r</i> -MMA)- <i>b</i> -PSt ( <b>B2</b> ) in CDCl <sub>3</sub> .	... p4
<b>Fig. S8</b> <sup>1</sup> H NMR spectrum of P(MAPhPOSS- <i>r</i> -MMA)- <i>b</i> -PSt ( <b>B4</b> ) in CDCl <sub>3</sub> .	... p4
<b>Fig. S9</b> <sup>1</sup> H NMR spectrum of P(MAPhPOSS- <i>r</i> -DEGMA)- <i>b</i> -PSt ( <b>B5</b> ) in CDCl <sub>3</sub> .	... p5
<b>Fig. S10</b> <sup>1</sup> H NMR spectrum of P(MAPhPOSS- <i>r</i> -HEMA)- <i>b</i> -PSt ( <b>B6</b> ) in CDCl <sub>3</sub> .	... p5
<b>Fig. S11</b> Photo of the block copolymer ( <b>B3</b> ) gel swollen with THF. The gel was prepared by mixing <b>B3</b> with TBAF and BTSB in THF followed by the evaporation of the solvent.	... p6
<b>Fig. S12</b> FT-IR spectra of (a) OctaphenylPOSS, (b) OctaphenylPOSS after the reaction with TBAF in THF, and (c) OctaphenylPOSS after the reaction with TBAF and the subsequent thermal annealing.	... p7
<b>Fig. S13</b> <sup>29</sup> Si CP/MAS NMR spectra of (a) OctaphenylPOSS, (b) OctaphenylPOSS after the reaction with TBAF in THF, and (c) OctaphenylPOSS after the reaction with TBAF and the subsequent thermal annealing.	... p7
<b>Fig. S14</b> <sup>13</sup> C CP/MAS NMR spectra of (a) <b>B3</b> , (b) <b>B3</b> after the cross-linking with TBAF and BTSB in THF, and (c) <b>B3</b> after the cross-linking and the subsequent thermal annealing.	... p8
<b>Fig. S15</b> Lorentz-corrected SAXS profiles of (a) P(MAPhPOSS- <i>r</i> -DEGMA)- <i>b</i> -PSt ( <b>B5</b> ) after the thermal annealing and (b) <b>B5</b> after the cross-linking by drying the THF solution with TBAF and BTSB followed by the thermal annealing.	... p8

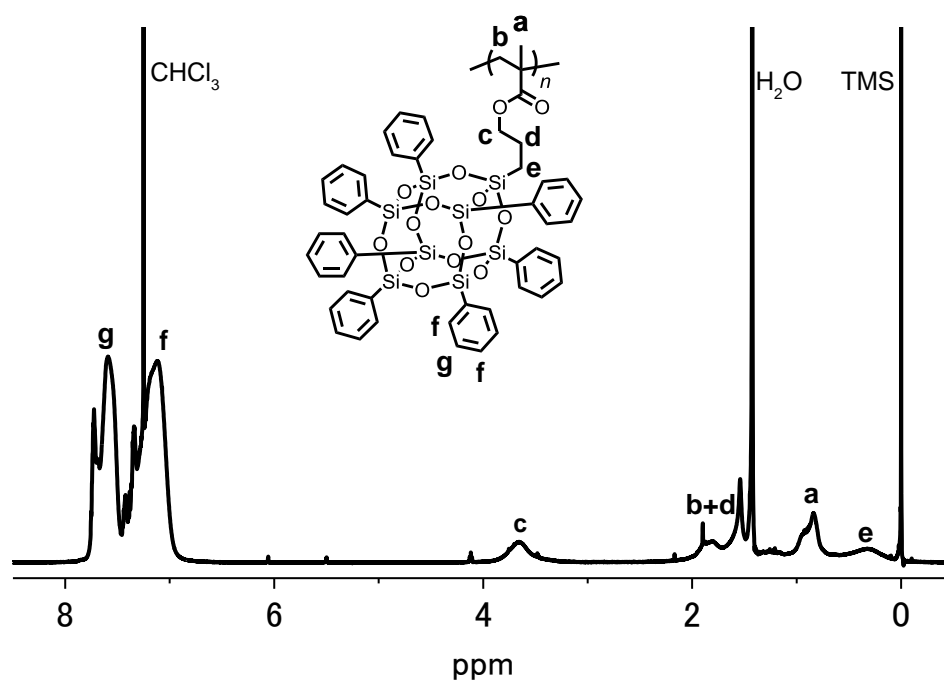


**Fig. S1**  $^1\text{H}$  NMR spectrum of PMAPhPOSS (**P1**) in  $\text{CDCl}_3$ .

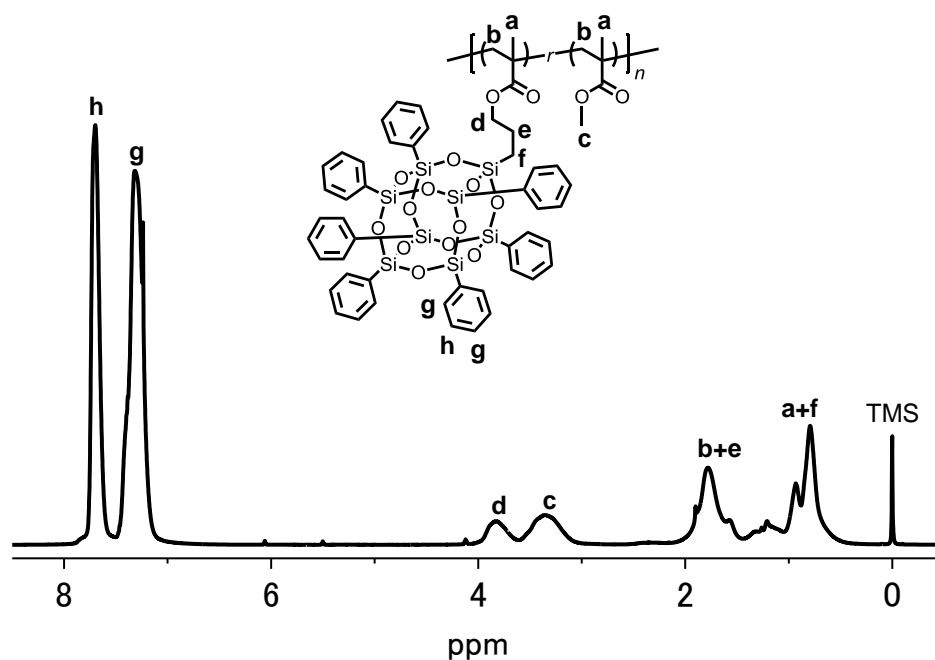


**Fig. S2**  $^1\text{H}$  NMR spectrum of P(MAPhPOSS-*r*-MMA) (**P2**) in  $\text{CDCl}_3$ .

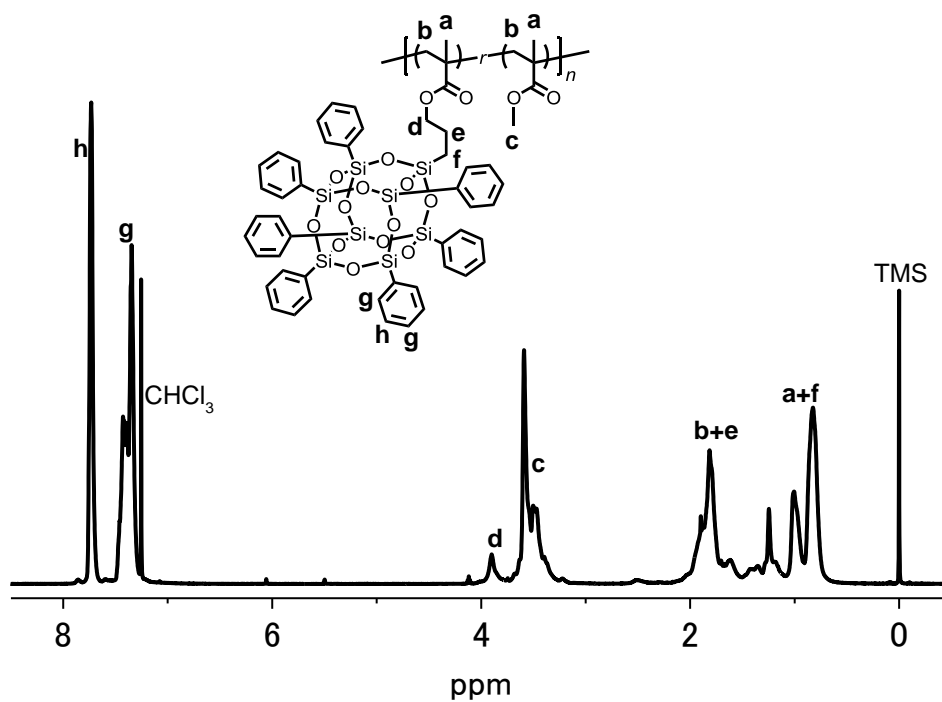


Fig. S3  $^1\text{H}$  NMR spectrum of P(MAPhPOSS-*r*-MMA) (P4) in  $\text{CDCl}_3$ .

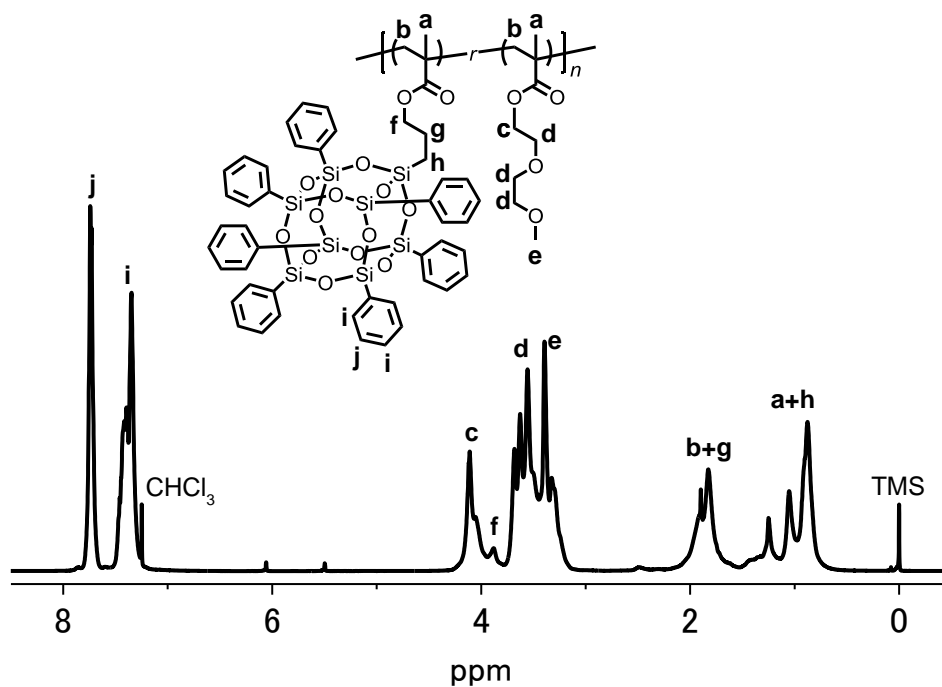


Fig. S4  $^1\text{H}$  NMR spectrum of P(MAPhPOSS-*r*-DEGMA) (P5) in  $\text{CDCl}_3$ .

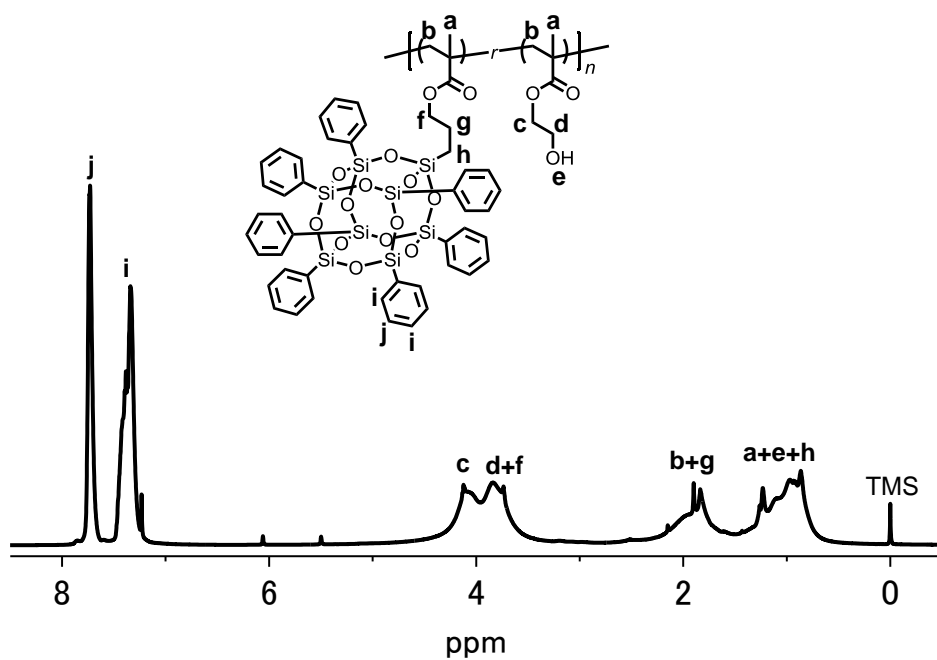


Fig. S5  $^1\text{H}$  NMR spectrum of P(MAPhPOSS-*r*-HEMA) (**P6**) in  $\text{CDCl}_3$ .

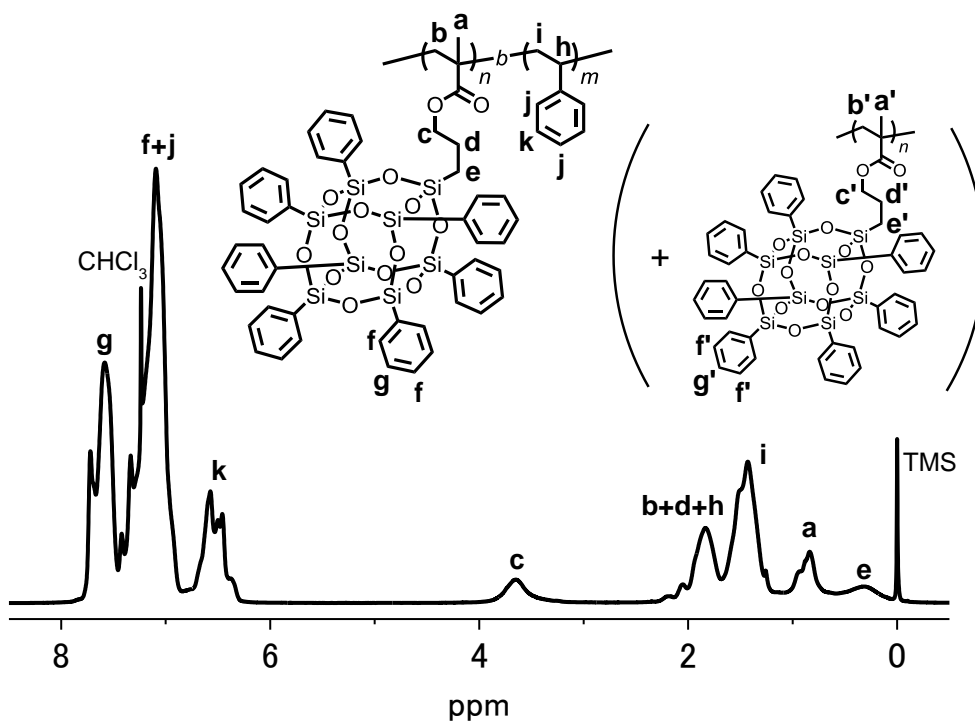


Fig. S6  $^1\text{H}$  NMR spectrum of PMAPhPOSS-*b*-PSSt (**B1**) in  $\text{CDCl}_3$ .

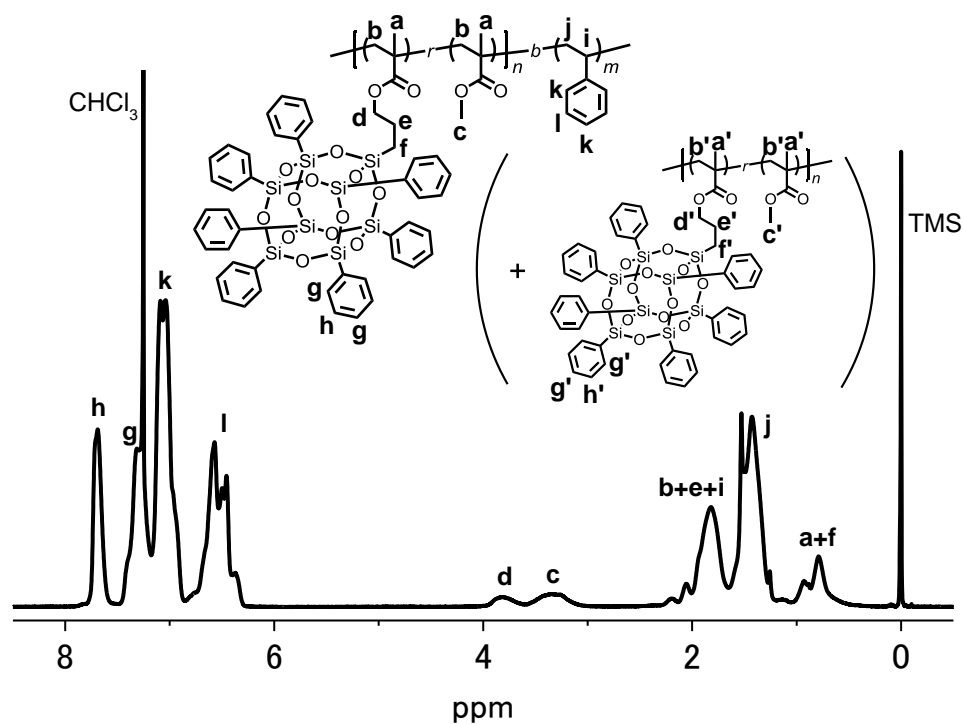


Fig. S7  $^1\text{H}$  NMR spectrum of P(MAPhPOSS-*r*-MMA)-*b*-PSt (**B2**) in  $\text{CDCl}_3$ .

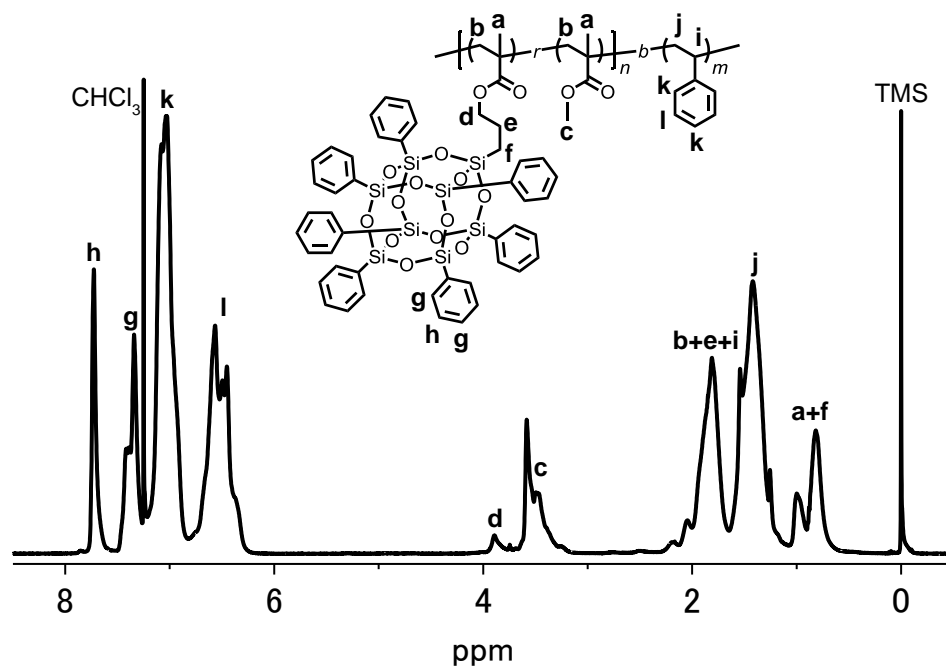
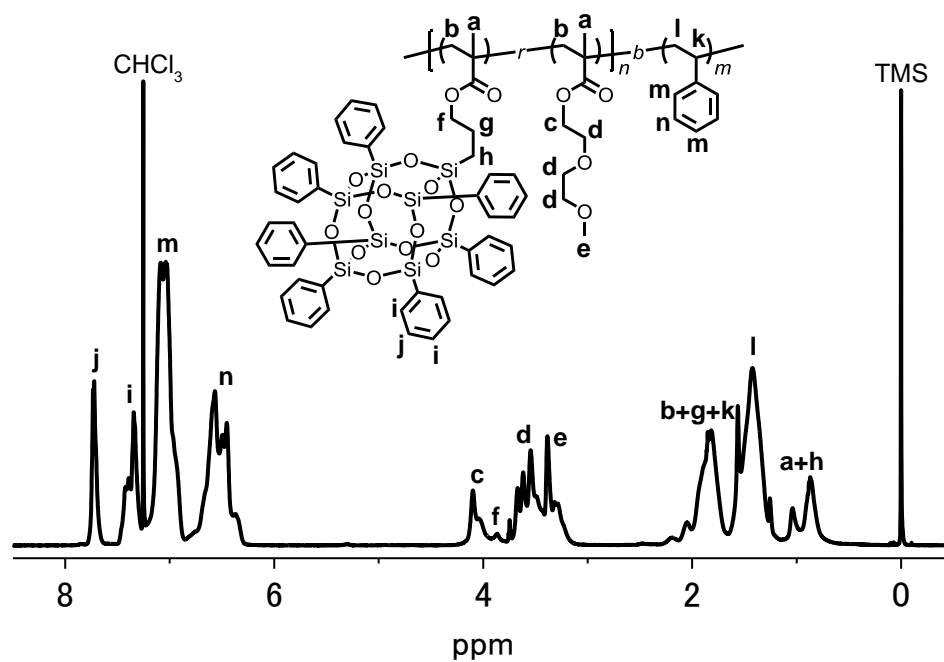
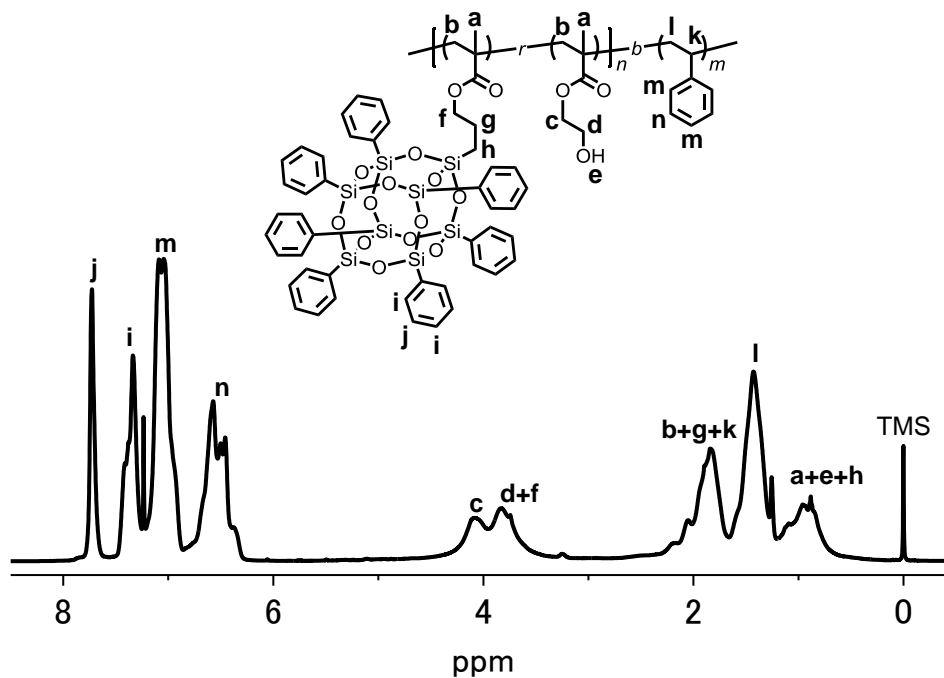


Fig. S8  $^1\text{H}$  NMR spectrum of P(MAPhPOSS-*r*-MMA)-*b*-PSt (**B4**) in  $\text{CDCl}_3$ .



**Fig. S9**  $^1\text{H}$  NMR spectrum of P(MAPhPOSS-*r*-DEGMA)-*b*-PSt (**B5**) in  $\text{CDCl}_3$ .



**Fig. S10**  $^1\text{H}$  NMR spectrum of P(MAPhPOSS-*r*-HEMA)-*b*-PSt (**B6**) in  $\text{CDCl}_3$ .

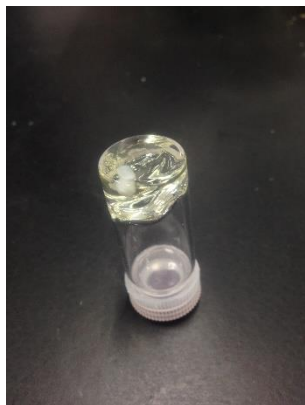


**Fig. S11** Photo of the block copolymer (**B3**) gel swollen with THF. The gel was prepared by mixing **B3** with TBAF (1 equiv. to POSS unit) and BTSE (0.5 equiv. to POSS unit) in THF (10 wt%) followed by the evaporation of the solvent (Run 1 in Table 3). The gel was insoluble in any common solvent for more than 1 week.

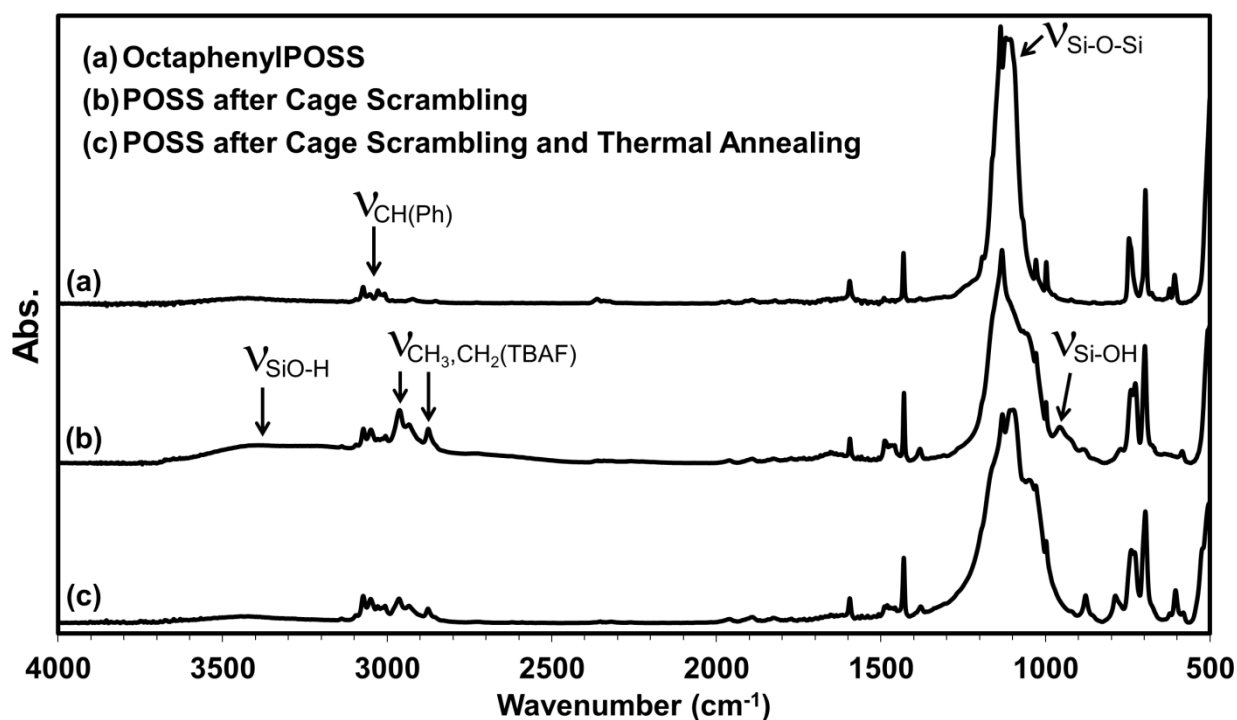


**Fig. S12** FT-IR spectra of (a) OctaphenylPOSS, (b) OctaphenylPOSS after the reaction with TBAF (1 equiv. to POSS) in THF (10 wt%), and (c) OctaphenylPOSS after the reaction with TBAF and the subsequent thermal annealing. at 150 °C for 120 h.

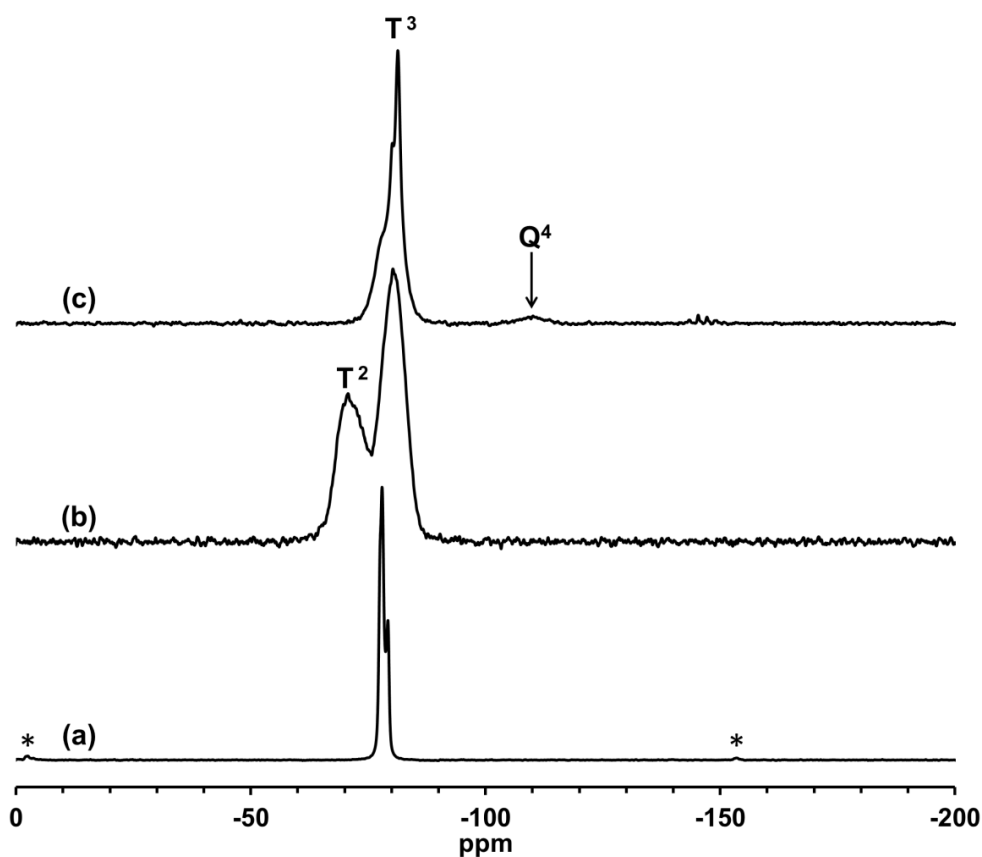


**Fig. S13**  $^{29}\text{Si}$  CP/MAS NMR spectra of (a) OctaphenylPOSS, (b) OctaphenylPOSS after the reaction with TBAF (1 equiv. to POSS) in THF (10 wt%), and (c) OctaphenylPOSS after the reaction with TBAF and the subsequent thermal annealing at 150 °C for 120 h. Peaks with \* are the spinning side bands of the main peak (6 kHz).

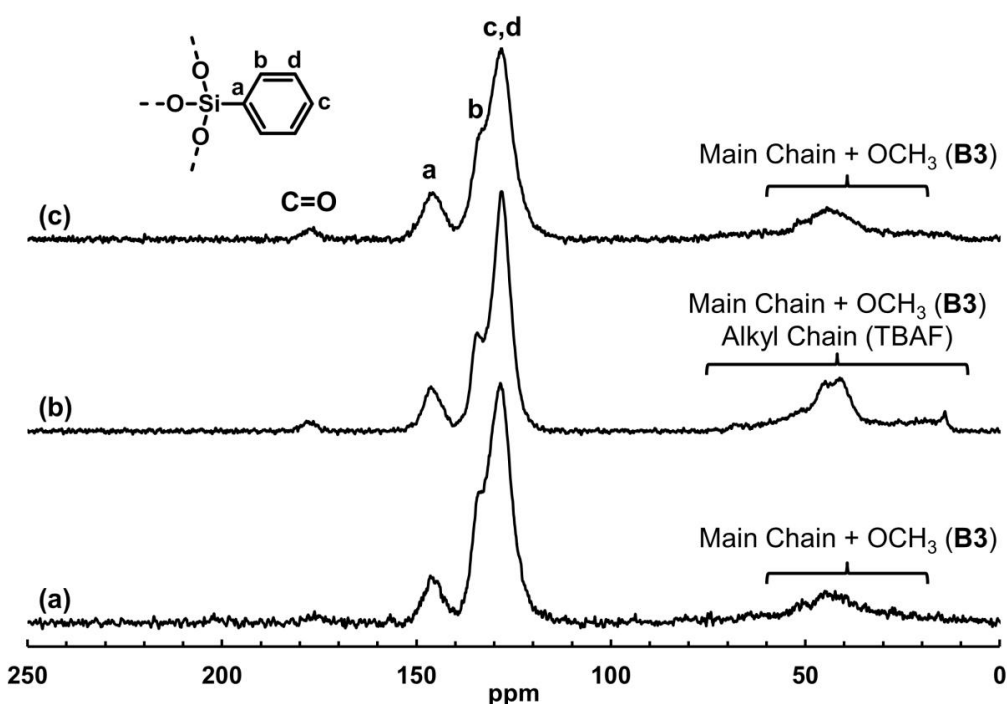


**Fig. S14**  $^{13}\text{C}$  CP/MAS NMR spectra of (a) **B3**, (b) **B3** after the cross-linking with TBAF (1 equiv. to POSS) and BTSB (0.5 equiv. to POSS unit) in THF (10 wt%), and (c) **B3** after the cross-linking and the subsequent thermal annealing. at 150 °C for 120 h.

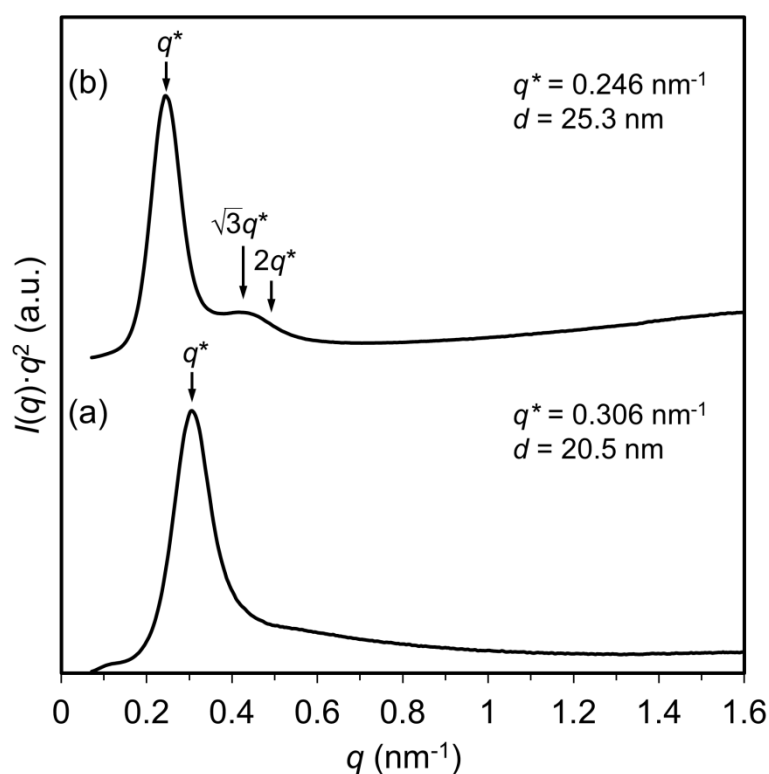


**Fig. S15** Lorentz-corrected SAXS profiles of (a) P(MAPhPOSS-*r*-DEGMA)-*b*-PSt (**B5**) after the thermal annealing and (b) **B5** after the cross-linking by drying the THF solution (10 wt%) with TBAF (1 equiv. to POSS unit) and BTSB (0.5 equiv. to POSS unit) followed by the thermal annealing. The thermal annealing condition was at 150 °C for 120 h under  $\text{N}_2$ .